Computational Methods for Differential Equations
http://cmde.tabrizu.ac.ir
Vol. 7, No. 3, 2019, pp. 383-395

Unknown functions estimation in a parabolic equation arises from Diffusion Tensor Magnetic Resonance Imaging

Fahimeh Soltanian*
Department of Mathematics, Payame Noor University,
P. O. Box 19395-3697, Tehran, Iran.
E-mail: f_soltanian@pnu.ac.ir

Morteza Garshasbi
Department of Mathematics, Iran University of Science
and Technology, P. O. Box 16846-13114, Tehran, Iran.
E-mail: m_garshasbi@iust.ac.ir

Abstract In this work, a general mathematical model of Diffusion Tensor Magnetic Resonance Imaging is formulated as an inverse problem. An effective numerical approach based on space marching method and mollification scheme is established to solve this problem. Convergence and stability of proposed approach are established. Using two test problems, the robustness and ability of the numerical approach is investigated.

Keywords. Inverse problem, Magnetic Resonance Imaging, Mollification, Regularized problem marching approach.

2010 Mathematics Subject Classification. 65M32, 65M12, 35K20.

1. Introduction

The recent introduction of Diffusion Tensor Magnetic Resonance Imaging (DT-MRI) has raised a strong interest in the medical imaging community. This non-invasive modality consists in measuring the water molecule motion within the tissues, using magnetic resonance techniques. The success of diffusion MRI is deeply rooted in the powerful concept that during their random, diffusion-driven displacements molecules probe tissue structure at a microscopic scale well beyond the usual image resolution. Many industrial and medical processes involve the flow of fluids through porous media. For instance the flow of blood through organ tissues and the transfer of gases to blood within the lung occur through porous materials. Usually the media are difficult to describe even on a local basis and properties vary spatially throughout the formations [5, 6, 14, 19, 20, 21].

An important aspect of the study of flow in porous materials is the nature of the fluids in pore space, which determines the mathematical characteristics of the model used to describe mechanical and thermodynamic phenomena associated with the flow. It is important to note that due to the relative inaccessibility of the fluid within the porous media, the properties of porous media typically have been inferred by

Received: 10 July 2018 ; Accepted: 30 September 2018.
* Corresponding author.

measuring fluid states outside of the porous media, and inferring properties within the porous media. The diffusion MRI can reveal orientation-dependent behavior of water molecules for localization of specific organs and pathologies, and for functionality assessment. As diffusion is truly a three dimensional process, molecular mobility in tissues may be anisotropic, as in brain white matter. With diffusion tensor imaging (DTI), diffusion anisotropy effects can be fully extracted, characterized, and exploited, providing even more exquisite details on tissue microstructure. On the other hand, measuring diffusion in the real space, for instance water diffusion in a living body, is not a simple task though it provides useful and important information. Indeed, incoherent motion of water molecules has certain anisotropy in living bodies relating to normal and abnormal structures [5, 6, 14, 19, 20].

The diffusion may be one of the most important and attractive notions in mathematical methods for image analysis. Diffusion equation is one of the most important models which appears in the MRI, and often is nonlinear. In this study a mathematical model which frequently arises in MRI is considered in a general form as a nonlinear parabolic initial-boundary value problem. One may find some theoretical and numerical results regard to these equations in spatial cases in literature [4, 11]. A mollified marching approach will be developed to solve this problem. The mollification method has been used for the stable numerical solution of a wide range of partial differential equations problems [1, 2, 3, 15, 16, 17]. This is due to the known fact that mollification is a reliable regularization procedure. More recently, it has been proved that mollification is a versatile and useful tool when dealing with parabolic equations and conservation laws [1, 18].

Our interest, inverse problem, is investigated numerically using a regularization method based on the discrete mollification method and space marching scheme. The mollification method can be used as a stabilizer of numerical schemes for a large class of partial differential equations (PDEs) such as parabolic and hyperbolic equations [1, 2, 3, 8, 9, 15, 16, 17, 18].

2. Description of the inverse problem

The effect of diffusion on the magnetic resonance signal has been discussed first by Hahn in 1950 [10] and later by Carr and Purcell in 1954 [7]. In 1956 Torrey incorporated these effects into the Bloch equations, creating the so-called Bloch-Torrey equation [7]

$$\frac{dM}{dt} = \mu(M \times B_0) + \Gamma(M_x, M_y, M_z, M_0) + D\nabla^2 M, \tag{2.1}$$

where M is the magnetization of an excited sample placed in a static magnetic field B_0, μ is the gyromagnetic ratio, M_x, M_y, M_z are the components of magnetization in the x, y, z directions, M_0 is the magnetization at thermal equilibrium T and D is the diffusion coefficient. In this study in the wake of Bloch-Torrey equation, following problem is discussed as an inverse problem of determination of unknown coefficient and boundary functions. Consider following problem

$$\begin{aligned} \frac{\partial M}{\partial t}(x,t) &= D\frac{\partial^2 M}{\partial x^2}(x,t) + \mu(x,t)F(M(x,t)) + f(x,t),\ (x,t)\in\Omega, && (2.2)\\ M_x(0,t) &= \psi(t),\ t\in\Lambda, && (2.3)\\ M_x(1,t) &= \gamma(t),\ t\in\Lambda, && (2.4)\\ M(x,0) &= g(x),\ x\in I, && (2.5) \end{aligned}$$

where $I=(0,1)$, $\Lambda=(0,T_f]$ and $\Omega = I\times\Lambda$. We assume that M is bounded positive function on Ω, $F(M)$ is a bounded Lipschitz continuous with Lipschitz coefficient λ, and $\mu(x,t)$ and $f(x,t)$ are bounded L^2-functions on Ω. In addition it is considered that all initial and boundary functions are continuous. For the existence and uniqueness of the solution of this problem, we refer the reader to [12, 13]. In the practical experiences, occasionally, the coefficient in the main equation and the boundary conditions or some parts of them may be unavailable due to physical situations. In this work, we consider the identification problem of the boundary function $\gamma(t)$ and coefficient function $\mu(x,t)$ in the problem (2.2)-(2.5) associated with known $\mu(0,t)$ and over-specified data

$$M(0,t) = \varphi(t),\ t\in\Lambda. \qquad (2.6)$$

In the sequence we will introduce a numerical marching scheme based on the mollification method (see [17]) to find the solution of the problem (2.2)-(2.6) under the assumption that $\psi(t)$, $\varphi(t)$ and $g(t)$ are only known approximately as $\psi^\varepsilon(t)$, $\varphi^\varepsilon(t)$ and $g^\varepsilon(x)$ such that

$$\begin{aligned} \|\psi(t)-\psi^\varepsilon(t)\|_\infty &\le \varepsilon, && (2.7)\\ \|\varphi(t)-\varphi^\varepsilon(t)\|_\infty &\le \varepsilon, && (2.8)\\ \|g(x)-g^\varepsilon(x)\|_\infty &\le \varepsilon. && (2.9) \end{aligned}$$

Owing to the presence of the noise in the problem's data, first, the problem will be stabilized using the mollification method.

3. Regularized problem and the marching scheme

To represent the regularized form of the problem (2.2)-(2.6), let us review briefly the discrete mollification. Let $\delta>0$, $p>0$, $A_p = (\int_{-p}^{p}\exp(-s^2)ds)^{-1}$, $Z=\{1,2,\cdots,M\}$, and $I_\delta = [p\delta, 1-p\delta]$. Notice that the interval I_δ is nonempty whenever $p<1/2\delta$.

Furthermore suppose $K=\{x_j : j\in Z\}\subset \overline{I} = [0,1]$, satisfying

$$x_{j+1}-x_j > d > 0, j\in Z, \qquad (3.1)$$

and

$$0\le x_1 < x_2 < \cdots < x_M \le 1, \qquad (3.2)$$

where d is a positive constant. Now if $G=\{g_j\}_{j\in Z}$ be a discrete function defined on K and $s_0 = s_M = 0$ and $s_j = (1/2)(x_j + x_{j+1})$, $1\le j\le M-1$, then the discrete

$\delta-$mollification of G is defined by [16]

$$J_\delta G(x)=\sum_{j=1}^{M}\left(\int_{s_{j-1}}^{s_j}\rho_{\delta,p}(x-s)ds\right)g_j, \tag{3.3}$$

where

$$\rho_{\delta,p}(x)=\begin{cases} A_p\delta^{-1}\exp\left(-\frac{x^2}{\delta^2}\right), & |x|\le p\delta,\\ 0, & |x|>p\delta.\end{cases} \tag{3.4}$$

Now the regularized form of the problem (2.2)-(2.6) may be written as follows

$$\begin{aligned} v_t(x,t) &= Dv_{xx}(x,t)-\mu(x,t)F(v(x,t))+f(x,t),\ (x,t)\in\Omega, && (3.5)\\ v(0,t) &= J_{\delta_1}\psi(t),\ t\in W, && (3.6)\\ v_x(0,t) &= J_{\delta_2}\varphi(t),\ t\in W, && (3.7)\\ v(x,0) &= J_{\delta_3}g(x),\ x\in I. && (3.8)\end{aligned}$$

The main goal of this problem is to determine $(v(x,t),\mu(x,t))\in\Omega$. Using the solution of this problem one may easily find the boundary function $\gamma(t)$. General cross validation (GCV) methods are used to choose the radii of mollification such as δ_1, δ_2 and δ_3 and others which will be used in the sequence [16, 17, 18]. With the sake of easiness, we consider $T_f=1$. To construct a numerical approach, assume P and N are positive integers and $h=\Delta x=1/P$ and $k=\Delta t=1/N$. Let us denote the discrete computed approximations of $v(ih,nk)$, $v_t(ih,nk)$, $v_x(ih,nk)$, $v_{xx}(ih,nk)$, $F(v(ih,nk))$, $\mu(ih,nk)$ and $f(ih,nk)$ by $U_{i,n}$, $W_{i,n}$, $Q_{i,n}$, $R_{i,n}$, $F_{i,n}$, $\mu_{i,n}$ and $f_{i,n}$ respectively. Using these notations, we introduce following space marching method

(1) Chose δ_0, δ_0^* and δ'.

(2) Find mollification of ψ^ε,φ^ε and g^ε in the interval $[0,1]$.
$U_{0,n}=J_{\delta_0}\psi^\varepsilon(nk)\ (n\neq 0)$, $\quad U_{i,0}=J_{\delta'}g^\varepsilon(ih),\ i\in\{0,1,\dots,P\}$,
$Q_{0,n}=K(0)J_{\delta_0^*}\varphi^\varepsilon(nk)$.

(3) Compute mollified differentiation in time (see section 3 of [15]) of $J_{\delta_0}\psi^\varepsilon(nk)$. Set
$W_{0,n}=\mathbf{D}_t(J_{\delta_0}\psi^\varepsilon(nk))\ (n\neq 0)$, $\quad W_{0,0}=\mathbf{D}_t(J_{\delta_0'}g^\varepsilon(0))$,
where $\mathbf{D}$ denotes the centered difference operator, i.e., $\mathbf{D}\eta(x)=\frac{\eta(x+\Delta x)-\eta(x-\Delta x)}{2\Delta x}$.

(4) Initialize $i=0$. Do while $i\le P-1$,

$$\begin{aligned} U_{i+1,n} &= U_{i,n}+hQ_{i,n},\ n\neq 0, && (3.9)\\ Q_{i+1,n} &= Q_{i,n}+\frac{h}{D}\left(W_{i,n}-\mu_{i,n}F_{i,n}-f_{i,n}\right), && (3.10)\\ W_{i+1,n} &= W_{i,n}+h\mathbf{D}_t(J_{\delta_i^*}Q_{i,n}), && (3.11)\\ R_{i+1,n} &= h\mathbf{D}_x(J_{\hat{\delta}_i^*}Q_{i+1,n}), && (3.12)\\ \mu_{i+1,n} &= \frac{1}{F_{i+1,n}}(W_{i+1,n}-DR_{i+1,n}-f_{i+1,n}). && (3.13)\end{aligned}$$

For a discrete function such as $X_{i,n}$, we suppose $|X_i|=\max_n|X_{i,n}|$. To prove the convergence and stability of proposed method assume that $v(x,t)\in C^2(I\times I)$.

4. Stability and convergence analysis

We analyze the convergence and stability of the proposed numerical scheme in this section. First consider

$$|\delta|_{-\infty} = \min_{1\leq i\leq P}(\delta', \delta_i, \delta_i^*, \hat{\delta}_i^*),$$
$$M_F = \max_u F(u),\ \ m_F = \min_u F(u),\ \ M_f = \max_{(x,t)\in[0,1]\times[0,1]}\{|f(x,t)|\}.$$

For the operator $\mathbf{D}$, one can prove that there exist a constant C where (Theorem 2 in [9])

$$|\mathbf{D}(J_\delta Q_{i,n})| \leq \frac{C}{|\delta|}|Q_{i,n}|. \tag{4.1}$$

Using (3.9)-(3.13) and (4.1) yields

$$|U_{i+1,n}| \leq (1+h)\max\{|U_{i,n}|, |Q_{i,n}|\}, \tag{4.2}$$

$$\begin{aligned}|W_{i+1,n}| &\leq |W_{i,n}| + \frac{hC}{|\delta|_{-\infty}}|Q_{i,n}| \\ &\leq \left(1+\frac{hC}{|\delta|_{-\infty}}\right)\max\{|Q_{i,n}|, |W_{i,n}|\},\end{aligned} \tag{4.3}$$

$$\begin{aligned}|Q_{i+1,n}| &\leq |Q_{i,n}| + h(|W_{i,n}| + M_F|\mu_{i,n}| + M_f) \\ &\leq (1+(2+M_F)h)\max\{|Q_{i,n}|, |W_{i,n}|, |\mu_{i,n}|, M_f\},\end{aligned} \tag{4.4}$$

$$|R_{i+1,n}| \leq \frac{hC}{|\delta|_{-\infty}}|Q_{i,n}|, \tag{4.5}$$

$$|\mu_{i+1,n}| \leq \frac{1}{m_F}\left((2+\frac{hC}{|\delta|_{-\infty}}+\frac{hCD}{|\delta|_{-\infty}}\right)\max\{|U_{i,n}|, |Q_{i,n}|, |W_{i,n}|, |\mu_{i,n}|, M_f\}. \tag{4.6}$$

Now suppose

$$C_\delta = \max\left\{1+h,\ \left(1+\frac{hC}{|\delta|_{-\infty}}\right),\ (1+(2+M_F)h,\ \frac{1}{m_F}\left((2+\frac{hC}{|\delta|_{-\infty}}+\frac{hCD}{|\delta|_{-\infty}}\right)\right\}.$$

Using (4.2)-(4.6) we can conclude that

$$\max\{|U_{i+1}|, |Q_{i+1}|, |W_{i+1}|, |\mu_{i+1}|\} \leq (1+hC_\delta)\max\{|U_i|, |Q_i|, |W_i|, |\mu_i|, M_f\},$$

and iterating this last inequality L times yields

$$\max\{|U_L|, |Q_L|, |W_L|, |\mu_L|\} \leq (1+hC_\delta)^L\max\{|U_0|, |Q_0|, |W_0|, |\mu_0|, M_f\}.$$

This inequality gives

$$\max\{|U_L|, |Q_L|, |W_L|, |\mu_L|\} \leq (\exp\ C_\delta)\max\{|U_0|, |Q_0|, |W_0|, |\mu_0|, M_f\}.$$

We can summarize the preceding analysis in the following statement.

Theorem 4.1 (The stability of the numerical solution)**.** *There exists a constant Λ, such that*

$$\max\{|U_L|, |Q_L|, |W_L|, |\mu_L|, M_f\} \leq \Lambda\max\{|U_0|, |Q_0|, |W_0|, |\mu_0|, M_f\}.$$

Proof. To prove this result, it is sufficient to assume $\Lambda = \exp \ C_\delta$ in the analysis preceding the statement of Theorem 4.1. □

To investigate the convergence of the proposed numerical method introduced in section 3, first suppose

$$\begin{aligned} \Delta U_{i,n} &= U_{i,n} - v(ih,nk), \quad \Delta Q_{i,n} = Q_{i,n} - v_x(ih,nk), \\ \Delta W_{i,n} &= W_{i,n} - v_t(ih,nk), \quad \Delta \mu_{i,n} = \mu_{i,n} - \mu(ih,nk). \end{aligned}$$

Taylor series yields some useful equations satisfied by the mollified solution v as follows

$$\begin{aligned} v((i+1)h,nk) &= v(ih,nk) + hv_x(ih,nk) + O(h^2), \\ v_x((i+1)h,nk) &= v_x(ih,nk) + v_{xx}(ih,nk) + O(h^2), \\ v_t((i+1)h,nk) &= v_t(ih,nk) + v_{x,t}(ih,nk) + O(h^2). \end{aligned}$$

Moreover we have

$$\begin{aligned} \Delta U_{i+1,n} &= \Delta U_{i,n} + (U_{i+1,n} - U_{i,n}) - (v((i+1)h,nk) - v(ih,nk)) \\ &= \Delta U_{i,n} + h(Q_{i,n} - v_x(ih,nk)) + O(h^2) \\ &= \Delta U_{i,n} + h\Delta Q_{i,n} + O(h^2), \end{aligned} \tag{4.7}$$

$$\begin{aligned} \Delta Q_{i+1,n} &= \Delta Q_{i,n} + (Q_{i+1,n} - Q_{i,n}) - (v_x((i+1)h,nk) - v_x(ih,nk)) \\ &= \Delta Q_{i,n} + h(R_{i,n} - v_{xx}(ih,nk)) + O(h^2) \\ &= \Delta Q_{i,n} + h(\mathbf{D}_x(J_{\hat{\delta}_i^*} Q_{i,n}) - v_{xx}(ih,nk)) + O(h^2), \end{aligned} \tag{4.8}$$

$$\begin{aligned} \Delta W_{i+1,n} &= \Delta W_{i,n} + (W_{i+1,n} - W_{i,n}) - (v_t((i+1)h,nk) - v_t(ih,nk)) \\ &= \Delta W_{i,n} + h(\mathbf{D}_t(J_{\delta_i^*} Q_{i,n}) - v_{xt}(ih,nk)) + O(h^2). \end{aligned} \tag{4.9}$$

Using $|\delta|_{-\infty}$, properties of discrete mollification (see [17, 18] for more details) and estimates (4.7)-(4.9) we find that there exist constants C, C_δ and C_{δ^*} such that

$$\begin{aligned} |\Delta U_{i+1,n}| &\leq |\Delta U_{i,n}| + h|\Delta Q_{i,n}| + O(h^2), \\ |\Delta Q_{i+1,n}| &\leq |\Delta Q_{i,n}| + h\left|\mathbf{D}_x(J_{\hat{\delta}_i^*} Q_{i,n}) - v_{xx}(ih,nk)\right| + O(h^2) \\ &\leq |\Delta Q_{i,n}| + h\left(C\frac{|\Delta U_{i,n}| + h}{|\delta|^2_{-\infty}} + C_\delta h^2\right) + O(h^2), \\ |\Delta W_{i+1,n}| &\leq |\Delta W_{i,n}| + h\left|\mathbf{D}_t(J_{\delta_i^*} V^n_{i,n}) - v_{tx}(ih,nk)\right| + O(h^2) \\ &\leq |\Delta W_{i,n}| + h\left(C\frac{|\Delta Q_{i,n}| + k}{|\delta|_{-\infty}} + C_{\delta^*} k^2\right) + O(h^2). \end{aligned}$$

So if we define

$$\begin{aligned}\Delta_i &= \max\{|\Delta U_{i,n}|, |\Delta W_{i,n}|, |\Delta Q_{i,n}|\},\\ C_0 &= \max\left\{1, \frac{C}{|\delta|_{-\infty}}, \frac{C}{|\delta|^2_{-\infty}}\right\},\\ C_1 &= \max\left\{\frac{h}{|\delta|^2_{-\infty}} + C_\delta h^2, \frac{Ck}{|\delta|_{-\infty}}, C_{\delta^*}k^2\right\},\end{aligned}$$

we have

$$\begin{aligned}\Delta_{i+1} &\leq (1+hC_0)\Delta_i + hC_1 + O(h^2)\\ &\leq (1+hC_0)(\Delta_i + C_1) + O(h^2),\end{aligned} \tag{4.10}$$

and finally after L iterations we obtain

$$\Delta_L \leq \exp(C_0)(\Delta_0 + C_1). \tag{4.11}$$

It is easy to see that if ε, h, and k tend to 0, then Δ_0 and C_1 tend to 0 too. Therefore $(\Delta_0 + C_1)$ and so does Δ_L tends to 0. Now define

$$H = \mu_{i+1,n}F_{i+1,n} - \mu((i+1)h, nk)F(v((i+1)h, nk)).$$

Then H may be written as

$$\begin{aligned}H &= \mu_{i+1,n}\left(F(v((i+1)h, nk)) - F_{i+1,n}\right)\\ &\quad + F(v((i+1)h, nk))\left(\mu_{i+1,n} - \mu((i+1)h, nk)\right)\\ &= \mu_{i+1,n}\Delta F_{i+1,n} + F(v((i+1)h, nk))\Delta\mu_{i+1,n},\end{aligned} \tag{4.12}$$

where $\Delta F_{i+1,n} = F(v((i+1)h, nk)) - F_{i+1,n}$. On the other hand using equations (3.5) and (3.13) we can write

$$H = \Delta W_{i+1,n} - D(\mathbf{D}_x(J_{\hat{\delta}_i^*}Q_{i+1,n}) - v_{xx}((i+1)h, nk)). \tag{4.13}$$

Using (4.12) and (4.13) yields

$$\begin{aligned}\Delta\mu_{i+1,n} &= \frac{1}{F(v((i+1)h, nk))}\{\Delta W_{i+1,n}\\ &\quad - D(\mathbf{D}_x(J_{\hat{\delta}_i^*}Q_{i+1,n}) - v_{xx}((i+1)h, nk)) - \mu_{i+1,n}\Delta F_{i+1,n}\}.\end{aligned} \tag{4.14}$$

Lipschitz continuity of F results in $|\Delta F_{i+1,n}| \leq \lambda|\Delta U_{i+1,n}|$. Therefore using (4.14) and (4.10) one may conclude that

$$\begin{aligned}|\Delta\mu_{i+1,n}| &\leq \frac{1}{m_F}\{|\Delta W_{i+1,n}| + hD(C\frac{|\Delta U_{i+1,n}| + h}{|\delta|^2_{-\infty}} + C_\delta h^2)\\ &\quad + \lambda M_\mu|\Delta U_{i+1,n}|\},\\ &\leq \frac{1}{m_F}\left(1 + \frac{hDC}{|\delta|^2_{-\infty}} + \lambda M_\mu\right)(\Delta_i + hC_1) + O(h^2),\end{aligned} \tag{4.15}$$

where $M_\mu = \max_\Omega |\mu(x,t)|$. Moreover

$$|\Delta\mu_{0,n}| = |J_{\delta_2}(\mu(0,t)) - \mu_{0,n}| \leq C(\varepsilon + k).$$

Using this fact and estimating (4.15), it is clear that as ε, h, and k tend to 0, $|\Delta\mu_{0,n}|$ and $|\Delta\mu_{i,n}|$ tend to 0 too.

The preceding analysis is summarized as following statement.

Theorem 4.2 (The convergence of the algorithm)**.** *For fixed δ as h, k and ε tend to zero, the discrete mollified solution converges to the mollified exact solution restricted to the grid points.*

Proof. See the analysis preceding this statement. □

5. Numerical experiments

To illustrate the validity of numerical approach presented in this study, two numerical examples are investigated in this section. We use GCV method to automatically determine the radii of mollification. To this end without loss of generality, we set $p = 3$ (see [16, 18]).

To generate Discretized approximate initial and boundary data, we add random errors to the exact initial and boundary functions. For example, for a sample function such as $\theta(x,t)$, its discrete noisy version can be generated as follows

$$\theta j, n^{\varepsilon} = \theta(x_j, t_n) + \varepsilon_{j,n}, \qquad j = 0, 1, \dots, N, n = 0, 1, \dots, T,$$

where $(\varepsilon_{j,n})$'s show Gaussian random variables with variance ε^2.

The exact solution of test problems are used to validate the accuracy of the numerical results. For comparison purpose between the numerical results and exact solutions, the l_2 relative weighted error norm is employed for instance for v as follows

$$\frac{\left[(1/(M+1)(N+1))\Sigma_{i=0}^{M}\ \Sigma_{j=0}^{N}|v(ih, jl) - U_{i,j}|^2\right]^{1/2}}{\left[(1/(M+1)(N+1))\Sigma_{i=0}^{M}\ \Sigma_{j=0}^{N}|v(ih, jl)|^2\right]^{1/2}}.$$

Example 1. *As the first test problem, in equations* (2.2)-(2.6) *suppose*

$$\psi(t) = e^t,\ \ \varphi(t) = e^t,\ \ g(x) = e^x,$$

$$F(M) = M,\ \ f(x,t) = -(t + x + 1)e^{x+t}.$$

The exact analytical solution of this problem is

$$M(x,t) = e^{x+t},\ \ \gamma(t) = e^{1+t}, \mu(x,t) = x + t + 1.$$

Table 1 reports the l_2 relative error norms of numerical results in four different noise levels for $M = N = 40, 100, 200, 300, 400$. The numerical results show that by decreasing the noise levels and increasing the number of mesh points, one may obtain more accurate results. Although for small noise levels step size h, the variation of l_2 relative error norms are not very sharp.

Figures 1, 2 and 3 demonstrate the behavior of relative l_2 error norms between exact and numerical results with respect to four different noise levels against the number of mesh points for M and N. It can be seen that decreasing the noise levels and increasing the number of mesh points, decrease the errors.

Table 1. Relative l_2 errors for Example 1.

ε	$M = N$	v	γ	μ
0.5	40	0.1905346	1.539593	1.000432
	100	0.0083546	0.1137237	0.0523191
	200	0.0038564	0.0786534	0.0711677
	300	0.0029696	0.0743575	0.0560709
	400	0.0025414	0.0708 731	0.0581105
0.1	40	0.0038534	0.0818543	0.0450453
	100	0.0024532	0.0791453	0.0387651
	200	0.0021432	0.0760543	0.0378121
	300	0.0022543	0.0712564	0.0366765
	400	0.0022576	0.0690987	0.0366342
0.01	40	0.00239865	0.0749242	0.0476321
	100	0.0023876	0.0710765	0.0361432
	200	0.0023765	0.0713876	0.0363432
	300	0.0023234	0.0712543	0.0366438
	400	0.0022311	0.0721654	0.0365876
0.001	40	0.0024654	0.0697543	0.0364657
	100	0.0022564	0.0691786	0.0363123
	200	0.0022231	0.0695543	0.0370129
	300	0.0022231	0.0694231	0.0365543
	400	0.0021786	0.0694763	0.0365349

Figure 1. The behavior of v's relative l_2 error norm for Example 1.

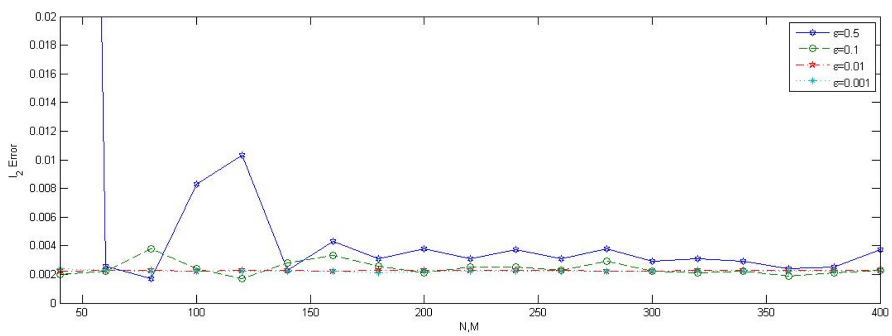

Example 2. *For the second test case, in equations* (2.2)-(2.6) *suppose*

$$\psi(t) = e^{-t}\sin(2) + 2,\ \varphi(t) = \cos(2)e^{-t},\ g(x) = \sin(x+2) + 2,$$

$$F(M) = M^2,\ f(x,t) = -(t^2x^2 + 1)(2 + e^{-t}\sin(x+2))^2.$$

FIGURE 2. The behavior of φ's relative l_2 error norm for Example 1.

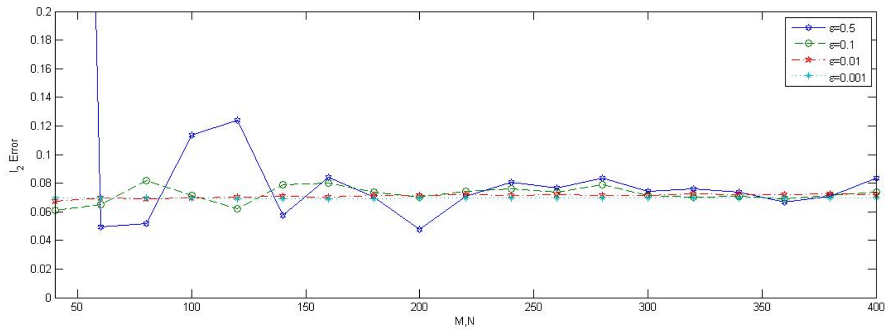

FIGURE 3. The behavior of μ's relative l_2 error norm for Example 1.

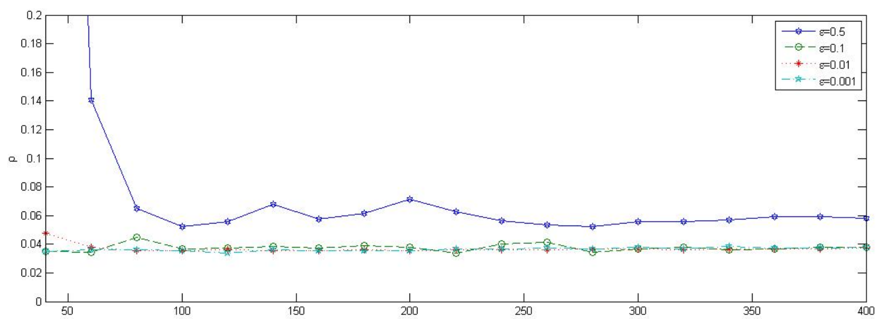

The exact analytical solution of this problem is

$$M(x,t) = e^{-t}\sin(x+2) + 2,\ \gamma(t) = e^{-t}\cos(x+2), \mu(x,t) = x^2t^2 + 1.$$

For v, γ and μ, the l_2 relative error norms between numerical and exact solutions in four different noise levels are shown for $M = N = 40, 100, 200, 300, 400$ in Table 2. As we expected, similar to the first test problem the numerical results show that by decreasing the noise levels and increasing the number of mesh points, one may obtain more accurate results.

Figures 4, 5 and 6 illustrate the relative l_2 error norms between exact and numerical results with respect to four different noise levels against the number of mesh points for M and N ($M = N$). It can be seen that decreasing noise levels and increasing the number of mesh points, decrease the errors. Similar to the first example when the number of mesh points increase, the variation of l_2 relative error norms are not very sharp.

TABLE 2. Relative l_2 errors for Example 2.

ε	$M = N$	v	γ	μ
	40	0.0.0057987	1.4108765	0.1904564
0.5	100	0.0044675	0.5838564	0.0946691
	200	0.0025891	0.0987056	0.0910984
	300	0.0022125	0.0567265	0.0771564
	400	0.0019819	0.0369261	0.0576505
	40	0.0016514	0.8292444	0.0622456
0.1	100	0.0015698	0.3167567	0.0543452
	200	0.0012147	0.0792656	0.0484456
	300	0.0011252	0.0688068	0.0477675
	400	0.0011435	0.0607579	0.0455313
	40	0.00160965	0.7485098	0.0648672
0.01	100	0.0014211	0.67603456	0.0514491
	200	0.0016145	0.09756787	0.0441595
	300	0.0012314	0.0726693	0.0498895
	400	0.0010471	0.0607655	0.0498215
	40	0.0015461	0.4764434	0.0642542
0.001	100	0.0014314	0.0987763	0.0547125
	200	0.00126781	0.0853763	0.0479297
	300	0.0011789	0.06578503	0.04801252
	400	0.0011987	0.0603725	0.0468948

FIGURE 4. The behavior of v's relative l_2 error norm for Example 2.

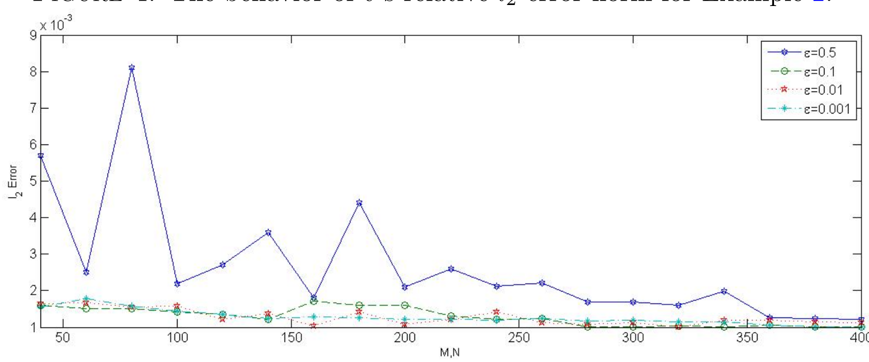

6. CONCLUSION

In this article, a mathematical model of Diffusion Tensor Magnetic Resonance Imaging (DT-MRI) is investigated as an inverse parabolic nonlinear diffusion problem. The regularized version of proposed model is used using mollification method. A numerical approach based on space marching scheme and mollification method is introduced to solve this inverse problem. Convergence and stability properties of this

Figure 5. The behavior of φ's relative l_2 error norm for Example 2.

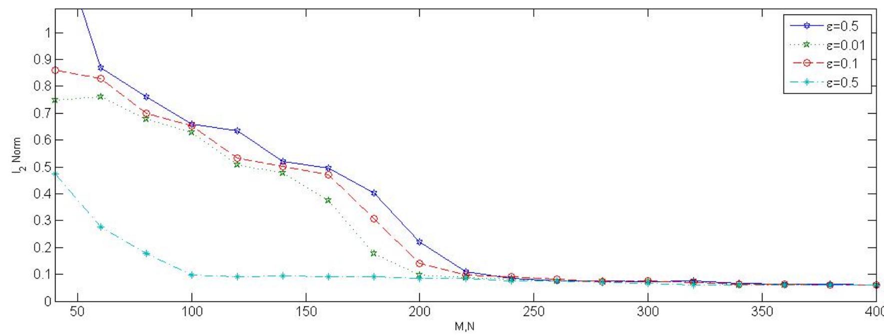

Figure 6. The behavior of μ's relative l_2 error norm for Example 2.

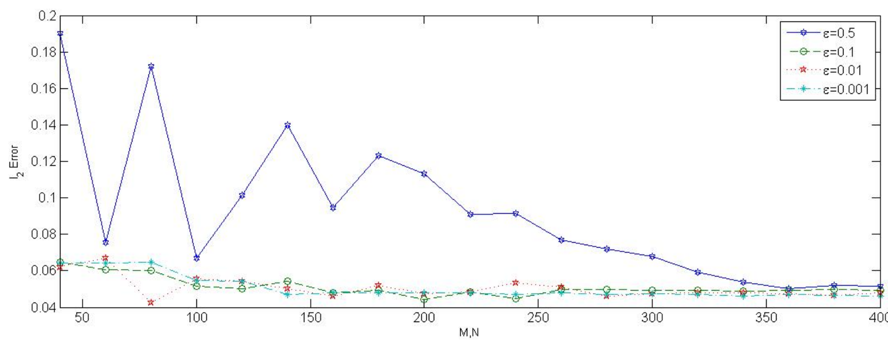

numerical method are proved which guarantee the reliability of numerical achievements. Implementation of this numerical method is very simple rather than other numerical techniques. Two test problems are conducted and numerical results are in good agreement with exact solutions.

References

[1] C. D. Acosta and C. E. Mejia, *Approximate solution of hyperbolic conservation laws by discrete mollification*, Appl. Numer. Math., *59* (2009), 2256–2265.

[2] C. D. Acosta and C. E. Mejia, *Stabilization of explicit methods for convection diffusion equations by discrete mollification*, Comput. Math. Appl., *55* (2008), 368–380.

[3] B. Anderssen, F. de Hogg, and M. Hegland, *A stable finite difference ansatz for higher order differentiation of nonexact data, Bull. Austral*, Math. Soc., *58* (1998), 223–232.

[4] S. N. Antontsev, A. V. Kazhikhov, and V. N. Monakhov, *Boundary value problems in mechanics of nonhomogeneous fluids*, North- Holland, Amsterdam, 1990.

[5] D. Le Bihan, E. Breton, and D. Lallemand, *MR imaging of intravoxel incoherent motions: application to diffusion and perfusion in neurologic disorders,* Radiology, *161* (1986), 401–407.

[6] D. Le Bihan and E. Breton, *Imagerie de diffusion in vivo par resonance magnetique nucleaire,* CR. Acad. Sci. Paris., *301* (1985), 1109–1112.

[7] H. Y. Carr and E. M. Purcell, *Effects of diffusion on free precession in nuclear magnetic resonance*, Phys. Rev., *94* (1954), 630–638.
[8] M. Garshasbi, P. Reihani, and H. Dastour, *A stable numerical solution of a class of semi-linear Cauchy problems*, J. Adv. Res. Dyn. Cont. Sys., *4* (2012), 56–67.
[9] M. Garshasbi and H. Dastour, *Estimation of unknown boundary functions in an inverse heat conduction problem using a mollified marching scheme*, Numer Algor., *68*(4) (2015), 769–790.
[10] E. L. Hahn, *Spin echoes*, Phys. Rev., *80* (1950), 580–594.
[11] P. Jenny, S. H. Lee, and H. A. Tchelepi, *Multi-scale finite-volume method for elliptic problems in subsurface flow simulation*, J. Comput. Phys., *187* (2003), 47–67.
[12] K. H. Karlsen and N. H. Risebro, *On the uniqueness and stability of entropy solutions of nonlinear degenerate parabolic equations with rough coefficients*, Discrete Contin. Dyn. Syst., *9* (2003), 1081–1104.
[13] G. M. Lieberman, *Second order parabolic differential equations*, World Scientific Publishing Co. Inc., River Edge, NJ, 1996.
[14] K.D. Merboldt, W. Hanicke, and J. Frahm, *Self-diffusion NMR imaging using stimulated echoes,* J. Magn. Reson., *64* (1985), 479–486.
[15] C. E. Mejia, D. A. Murio, and S. Zhan, *Some applications of the mollification method*, in: M. Lassonde (Ed.), App. Opti. Math. Eco., Physica-Verlag, 2001, 213–222.
[16] D. A. Murio and ZH. Yi, *Source term identification in 1-D IHCP*, Computers Math. Applic., *47* (2004), 1921–1933.
[17] D. A. Murio, *The mollification method and the numerical solution of ill-posed problems*, John Wiley and Sons, New York, 1993.
[18] D. A. Murio, *Mollification and space marching*, Chapter 4 in Inverse Engineering Handbook, (Edited by K. Woodbury), CRC Press, Boca Raton, FL, 2002.
[19] E. O. Stejskal and J. E. Tanner, *Spin diffusion measurements: spin echoes in the presence of a time-dependent field gradient,* J. Chem. Phys., *42* (1965), 288–292.
[20] D. G. Taylor and M. C. Bushell, *The spatial mapping of translational diffusion coefficients by the NMR imaging technique,* Phys. Med. Biol., *30* (1985), 345–349.
[21] H. C. Torrey, *Bloch equations with diffusion terms*, Phys. Rev., *104* (1956), 563–565.